Life Sciences 232 (2019) 116590

Contents lists available at ScienceDirect

Life Sciences

journal homepage: www.elsevier.com/locate/lifescie

MicroRNA-122 promotes endothelial cell apoptosis by targeting XIAP: Therapeutic implication for atherosclerosis

Yang Li, Ning Yang, Bo Dong, Jingyu Yang, Lu Kou, Qin Qin*

Department of Cardiology, Tianjin Chest Hospital, Tianjin 300222, China

ARTICLE INFO

Keywords:
MicroRNA-122
Endothelial cell
Apoptosis
XIAP
Atherosclerosis

ABSTRACT

Endothelial cell (EC) apoptosis is fundamental for the pathophysiology of atherosclerosis, in which microRNAs (miRNAs) emerge as critical regulators. miR-122 has been shown to regulate the apoptosis of various cell types, however, whether miR-122 is associated with atherosclerosis and EC apoptosis remains unknown. In this study, we found that miR-122 expression was increased in the aortic ECs of ApoE$^{-/-}$ mice fed with a high-fat diet (HFD), as compared to normal-diet (ND), implying a potential association between miR-122 elevation and atherogenesis. In addition, in vitro, miR-122 expression was also induced in human aortic ECs (HAECs) by the treatment of oxidized low-density lipoprotein (ox-LDL), a common atherogenic factor. Functionally, miR-122 knockdown suppressed ox-LDL-induced apoptosis of HAECs, suggesting a pro-apoptotic role of miR-122 in HAECs under this pro-atherogenic condition. Further evidence revealed that the X-linked inhibitor-of-apoptosis protein (XIAP) was directly targeted and suppressed by miR-122 in HAECs, and more importantly, XIAP knockdown diminished miR-122 effect on apoptosis, thus establishing XIAP as a prominent target that mediates miR-122 regulation of the apoptosis of HAECs. Together, these results may identify miR-122 as a novel regulator in EC apoptosis, which offers it as a possible target for therapeutic interventions of atherosclerosis.

1. Introduction

Atherosclerosis is a chronic vascular disorder of the arterial wall, which represents a major cause of many life-threatening diseases such as stroke, myocardial infarction and heart failure [1,2]. Although atherosclerosis is largely caused by the accumulation of lipids in the arterial wall, other risk factors are also actively involved in its pathogenesis, including endothelial dysfunction [3], macrophage accumulation [4], vascular smooth muscle cells (VSMCs) dedifferentiation [5], and production of inflammatory cytokines [6]. It's also established that the endothelial cell (EC) apoptosis plays vital roles in the initiation of atherosclerotic lesions through multiple mechanisms: 1) compromising the normal function of endothelium to dysregulate lipid homeostasis and inflammation [7–9]; 2) disrupting the integrity of endothelium to promote lipid deposition into atherogenesis [10]; 3) instabilizing plaque to predispose to arterial thrombosis [11]. The EC apoptosis can be induced by low-density lipoprotein (LDL), elevated blood glucose, reactive oxygen species (ROS)-mediated oxidative stress, and low shear stress [12]. Nonetheless, little is known about how EC apoptosis is regulated at the molecular level.

MicroRNAs (miRNAs) are small non-coding RNAs that regulate the expression of target genes posttranscriptionally [13]. Recently, several miRNAs have been shown to control EC apoptosis [14,15]. For example, miR-429 and miR-365 promote EC apoptosis by downregulating Bcl-2 expression [16,17]. In addition, miR-26a prevents EC apoptosis by directly targeting TRPC6 [18], and let-7c regulates ox-LDL-induced EC apoptosis via inhibiting Bcl-xl expression [19]. The regulation of EC apoptosis by miRNAs implicates their potentiality in modifying atherosclerosis progression.

Previous studies have reported that miR-122 regulates the apoptosis of a variety of cell types, such as hepatocellular carcinoma [20], T-cell lymphoma [21], gastric cancer cells [22], and cardiomyocytes [23]. However, to date, whether miR-122 is involved in EC apoptosis and associated with atherosclerosis are not characterized. Here, we report that miR-122 expression is increased in the aortic intima of mouse model of atherosclerosis, and that miR-122 promotes ox-LDL-induced apoptosis of HAECs by targeting XIAP. Thus, our study uncovers a potential connection between miR-122 and atherogenesis.

2. Materials and methods

2.1. Animals and atherosclerosis model

The apolipoprotein (apo) E is a major apoprotein essential for

* Corresponding author at: Department of Cardiology, Tianjin Chest Hospital, Tianjin 300222, No. 261 Taierzhuang South Road, Jinnan District, Tianjin, China.
E-mail address: cardioq@126.com (Q. Qin).

https://doi.org/10.1016/j.lfs.2019.116590
Received 24 April 2019; Received in revised form 17 June 2019; Accepted 18 June 2019
Available online 19 June 2019

catabolizing triglyceride-rich lipoprotein particles [24], and ApoE$^{-/-}$ transgenic mice display atherosclerotic lesions similar to those in humans, which makes them to be ideal animal models for investigating atherosclerosis [25]. In this study, twelve-week-old male ApoE$^{-/-}$ mice were purchased from the Jackson Laboratory (Bar Harbor, ME, USA) and maintained under a standard animal facility. Mice were randomly divided into normal diet (ND) group and high-fat diet (HFD) group. Each group contains 6 mice. The high-fat diet is comprised of 1% cholesterol, 3% lard, 10% yolk powder and 86% normal diet, which were purchased from the Beijing HFK Bioscience Co. Ltd., Beijing, China. Mice in HFD group were feed a diet with high fat ad libitum for 16 weeks to induce atherosclerosis as previously described [18]. The pathologic examination of atherosclerosis was performed by staining the aortic root with HE to visualize the atherosclerotic lesions [18]. All animal experimental procedures were performed in accordance with the guideline approved by the Animal Care and Use Committee of Tianjin Chest Hospital for the welfare of laboratory animals.

2.2. Isolation of aortic intima and endothelial cells

The isolation of aortic intima from the whole aorta was conducted as described previously [26]. In brief, mice were transcardially perfused with cold saline, and then aortas were exposed and the surrounding tissues were removed carefully. After removing perivascular fat, thoracic aorta was removed and transferred into a dish with ice-cold saline. Aorta was cut through and intima was carefully stripped from aorta. The excised aortic intima was washed twice with PBS, minced and digested with 2% collagenase (Sigma-Aldrich) for 40 min to obtain endothelial cells, which were collected by centrifugation and used for following extraction of RNA and protein.

2.3. Cell culture, treatment and transfection

HAECs were purchased from ScienCell Research Laboratories (Carlsbad, CA, USA), and cultured in Endothelial Cell Growth Medium (Sigma-Aldrich, 211-500) added with Endothelial Cell Growth Supplement (ECGS) (BD Biosciences, 354006-356006), 10% fetal bovine serum (Invitrogen) and 1% penicillin/streptomycin (ThermoFisher Scientific, 15140122). HAECs were maintained at 37 °C in an incubator with 5% CO_2. To establish in vitro apoptosis model induced by ox-LDL, HAECs were treated with ox-LDL (Invitrogen, L34357) at different concentrations (25, 50, 100 μg/ml) according to our pilot experiments. The transient transfection of HAECs by miR-122 mimic or miR-NC, or siNC or siXIAP, was performed using Lipofectamine 2000 reagent (ThermoFisher Scientific) according to the manufacturer's instructions. The sequences of NC mimic, miR-122 mimic, NC inhibitor, and miR-122 inhibitor were described in a previous study [27], and synthesized by GenePharma (Shanghai, China).

2.4. Real-time quantitative PCR analysis

The total RNAs were isolated from cells using TRIzol reagent (Invitrogen) according to the manufacturer's instructions. The isolated total RNAs were reversely transcribed into complementary cDNAs using SuperScrip IV One-Step RT-PCR System (Invitrogen, 12594100). cDNAs were used as templates for real-time quantitative PCR (RT-qPCR) analysis to quantify the expression of miR-122, for which U6 was used as an internal control. Data were presented as values calculated by $2^{-\triangle\triangle Ct}$ method [28]. The sequences of primers for amplifying miR-122 and U6 were previously descried [29]. The sequences of primers for amplifying XIAP and β-actin are listed as follows: XIAP, 5′-CTTGAGGAGTGTCTG GTAAG-3′ and 5′-GTGACTAGATGTCCACAAGG-3′. β-actin, 5′-AGCCA TGTACGTAGCCATCC-3′ and 5′-CTCTCAGCTGTGGTGGTGAA-3′.

2.5. Western blotting analysis

Western blotting analysis was conducted as described previously [30]. Briefly, cells were lysed in RIPA lysis buffer (Beyotime) supplemented with protease inhibitor Cocktail (Sigma-Aldrich). Protein samples were collected, separated by SDS-PAGE and transferred to nitrocellulose (NC) membranes, which were blocked with 5% non-fat milk, and then probed with primary antibodies overnight at 4 °C, followed by incubation with HRP-labeled secondary antibodies for 1 h at room temperature. Protein blots were visualized using Pierce Enhanced Chemiluminescence Reagent (ThermoFisher Scientific). Antibodies were purchased from the following sources: anti-VEGFR2 (Sigma-Aldrich, SAB4501645), anti-SM22 (Proteintech, 10493-1-AP), anti-calponin (Santa Cruz, sc-58707), and anti-cleaved caspase-3 (Cell Signaling Technology, 9664), anti-XIAP (Abcam, ab21278) and anti-β-actin (Abcam, 8227). The intensity of protein blots was analyzed by Image J software [31].

2.6. Apoptosis detection

Cell apoptosis was detected by the terminal deoxynucleotidyl transferase (TdT) terminal deoxynucleotidyl transferase (TdT) dUTP nick-end labeling (TUNEL), which identifies the blunt ends of double-stranded DNA breaks by TdT, an enzyme catalyzing the addition of labeled dUTPs to a 3′-hydroxyl termini of DNA ends, permitting final visualization using immunohistochemical techniques [32]. HAECs were seeded on coverslips in 24-well plates. After treatment, cells were fixed with 4% paraformaldehyde and permeabilized with 0.1% Triton X-100. Then, TUNEL staining was performed using TUNEL fluorescence FITC kit (Roche, Indianapolis, IN, USA) according to the manufacturer's protocols. Cells were counterstained with DAPI to visualize nuclei, and the stained cells were imaged under FV300 confocal microscope (Olympus, Japan). Fifteen random fields were counted for each treatment. Cell apoptosis was analyzed as the percentage of TUNEL-positive cells within total number of cells. Moreover, the apoptosis of aortic ECs was also detected by the Annexin V/PI staining as previously described [33].

2.7. Luciferase reporter assay

Luciferase reporter assay was conducted as described in a previous study [34]. In brief, the wild-type (5′…CUUAAAAUCACUCAG**CACUC**C**A**A…3′) and mutant (5′…CUUAAAAUCACUCAG**GUGCGA**AA… 3′) 3′UTR of XIAP was individually inserted into the luciferase reporter psi-CHECK2 plasmids (Promega, Madison, WI, USA). HEK293 cells were seeded in 24-well plates and co-transfected wild-type or mutated luciferase reporter plasmids along with miR-122 or miR-NC, or anti-miR-122 or anti-miR-NC using Lipofectamine 2000 reagent (ThermoFisher Scientific). Cells were harvested following 48 h of transfection. Luciferase activities were assessed using Dual-Luciferase Reporter Assay System (Promega) following manufacturer's instructions. The activity of Renilla luciferase was set as an internal control.

2.8. Statistical analysis

Data were shown as the mean ± standard deviation (SD). Comparisons between two groups were analyzed by Student's *t*-test, and comparisons among more than two groups were analyzed by one-way ANOVA followed by post-hoc Turkey's test. $P < 0.05$ was considered statistically significant for all analyses.

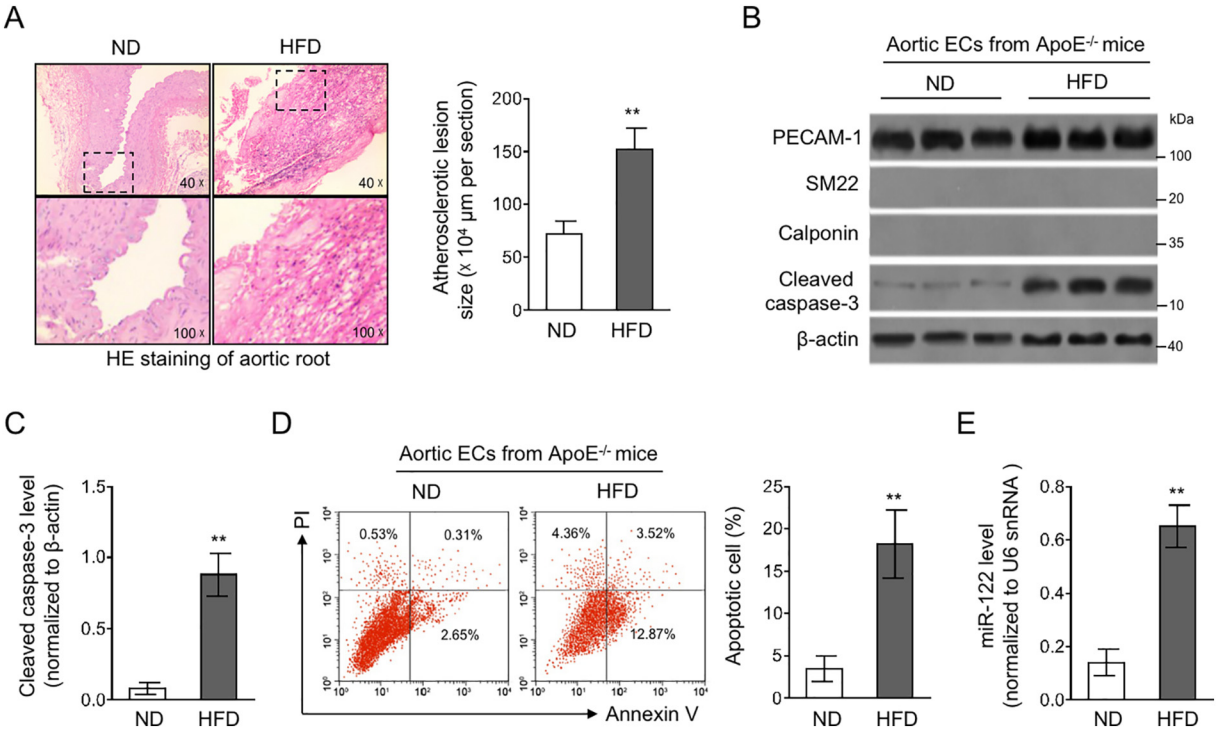

Fig. 1. miR-122 expression is elevated in HAECs from the aortic intima of ApoE$^{-/-}$ mice fed with HFD.
(**A**–**E**) ApoE$^{-/-}$ mice were fed a high-fat diet (HFD) or normal diet (ND) for 16 weeks. Each group includes 6 mice. (**A**) The aortic root sections were analyzed by HE staining. The representative images of each group were presented (left) and the quantification analysis of the atherosclerotic lesion size was also shown (right). (**B**) The aortic intima of ApoE$^{-/-}$ mice was isolated and analyzed by Western blotting to determine the protein expression of endothelia marker PECAM-1, smooth muscle cell markers SM22 and calponin 1, and apoptotic marker cleaved caspase-3. β-actin was used as a loading control. Blot images were representative of 3 mice in each group. (**C**) The level of cleaved caspase-3 expression was quantified and normalized to that of β-actin. (**D**) The apoptosis of aortic ECs isolated from the aortic intima was determined by the Annexin V/PI staining analysis. The percentage of apoptotic cells (Annexin V^{+}) was shown. (**E**) miR-122 expression in the aortic intima isolated from ApoE$^{-/-}$ mice was determined by qRT-PCR analysis. U6 snRNA was used as a reference control. Data are expressed as mean ± SD ($n = 6$). Student's *t*-test. $^{**}P < 0.01$ vs. ND.

3. Results

3.1. miR-122 is induced in the aortic endothelial cells of ApoE$^{-/-}$ mice fed with HFD

To test whether there exists a possible link between miR-122 and endothelial cell (EC) apoptosis taking place in the process of atherogenesis, a widely-used experimental atherosclerosis model was developed in ApoE$^{-/-}$ mice by feeding a high-fat diet (HFD) for 16 weeks, and then, aortic endothelial cells (ECs) were isolated from the aortic intima of ApoE$^{-/-}$ mice for detecting the expression of miR-122 and apoptotic marker cleaved caspase-3. ApoE$^{-/-}$ mice fed a normal diet (ND) were used as controls. First, the successful induction of atherosclerosis in HFD-fed ApoE$^{-/-}$ mice was validated by the increased atherosclerotic lesions, as revealed by HE staining of the aortic root (Fig. 1A). Then, the purity of isolated aortic ECs was confirmed by the enriched expression of surface protein marker PECAM-1 and the absent expression of smooth muscle cell (SMC) marker SM22 and calponin 1 (Fig. 1B) [35]. HFD is known to induce the apoptosis of ECs in ApoE$^{-/-}$ mice [36,37]. Consistently, we found that in contrast to ND group, the expression of cleaved caspase-3, a marker of apoptosis [38], was drastically elevated in aortic ECs from ApoE$^{-/-}$ mice fed HFD (Fig. 1B-C). The increased apoptosis of aortic ECs in HFD-fed ApoE$^{-/-}$ mice was further proven by the Annexin V/PI double staining assay (Fig. 1D). Meanwhile, qRT-PCR analysis showed that the expression level of miR-122 was significantly induced in aortic ECs from ApoE$^{-/-}$ mice fed HFD (Fig. 1E). Altogether, these results suggest that the apoptosis of aortic ECs is induced in ApoE$^{-/-}$ mice fed HFD and miR-122 expression is simultaneously upregulated, which implies that miR-122 may be involved in EC apoptosis in the context of atherosclerosis.

3.2. miR-122 is induced in HAECs treated with ox-LDL

We next checked miR-122 expression in ECs by applying an in vitro system, in which human aortic endothelial cells (HAECs) were treated with oxidized low-density lipoprotein (ox-LDL), an atherogenic factor that is thought to play a central role during atherogenesis and capable of inducing EC apoptosis [39,40]. As expected, ox-LDL treatment dose-dependently induced the apoptosis of HAECs, as shown by increased expression of cleaved caspase-3 (Fig. 2A). In addition, in these ox-LDL-treated HAECs, the expression of miR-122 was also markedly induced (Fig. 2B). Moreover, the expression levels of cleaved caspase-3 (Fig. 2C) and miR-122 (Fig. 2D) were synchronously increased in HAECs by ox-LDL treatment in a time-dependent manner. Collectively, these data point to a positive association between miR-122 expression and apoptosis induction in ox-LDL-treated HAECs, which is reminiscent of miR-122 upregulation in aortic ECs from ApoE$^{-/-}$ mice with atherosclerosis induced by HFD.

3.3. Inhibition of miR-122 suppresses apoptosis of HAECs induced by ox-LDL

miR-122 regulates apoptosis in cancer cells and cardiomyocytes [20,21,41], however it's unknown whether miR-122 affects ox-LDL-induced apoptosis in HAECs. In order to address this issue, we inhibited miR-122 in ox-LDL-treated HAECs by transfecting antisense oligonucleotides (miR-122 inhibitor) (Fig. 3A). The apoptosis of HAECs was then assessed by TUNEL assay, which showed that the extent of ox-LDL-

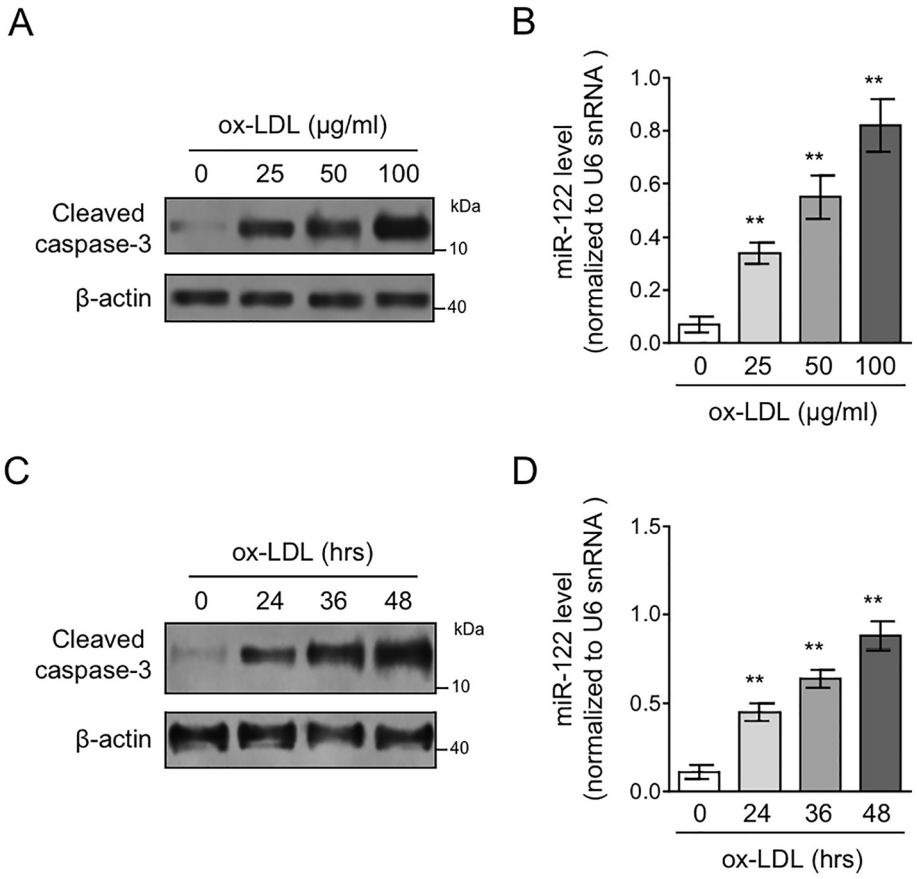

Fig. 2. miR-122 expression is elevated in HAECs treated with ox-LDL.
(**A–B**) HAECs were treated with increasing concentrations of ox-LDL for 2 days as indicated. (**A**) The protein expression of cleaved caspase-3 was determined by Western blotting analysis. β-actin was used as a loading control. Representative images from 3 independent assays are depicted. (**B**) miR-122 expression was determined by qRT-PCR analysis. U6 snRNA was used as a reference control. (**C–D**) HAECs were treated with 100 μg/ml ox-LDL for increasing time periods. The expression levels of cleaved caspase-3 (**C**) and miR-122 (**D**) were analyzed as in (A–B). Data are expressed as mean ± SD ($n = 3$). One-way ANOVA followed by post-hoc Turkey's test. $^{**}P < 0.01$ vs. control.

induced apoptosis in HAECs was significantly attenuated when transfected with miR-122 inhibitor, as compared with negative control (NC) inhibitor (Fig. 3B), indicating that miR-122 knockdown reduces ox-LDL-induced apoptosis in HAECs. Additionally, in accordance with this result, ox-LDL-induced expression of cleaved caspase-3 was also decreased by miR-122 inhibitor (Fig. 3C), further confirming the anti-apoptotic function of miR-122 knockdown in ox-LDL-treated HAECs. Altogether, these findings suggest that miR-122 may serve as a positive regulator of EC apoptosis induced by atherogenic factors.

3.4. miR-122 targets XIAP in HAECs

To understand how miR-122 regulates ox-LDL-induced apoptosis in HAECs, we took advantage of TargetScan algorithm (http://www.targetscan.org) to predict potential targets of miR-122. Among these predicted candidates, the X chromosome-linked inhibitor of apoptosis (XIAP) attracted our attention due to its critical role in the regulation of apoptosis by binding and inhibiting caspases (Fig. 4A) [42]. To examine whether XIAP contributes to miR-122 regulation of ox-LDL-induced apoptosis in HAECs, we first verified whether XIAP is a direct target of miR-122 through conducting luciferase reporter assay. As shown, miR-122 overexpression in HEK293 cells strikingly reduced the luciferase activity of wild-type XIAP construct, but did not have similar effect on that of the mutant XIAP construct (Fig. 4B). Conversely, miR-122 knockdown significantly increased the luciferase activity of wild-type XIAP construct, and no similar effect was observed for the mutant XIAP construct either (Fig. 4C). Hence, these observations indicate that miR-122 directly targets the mRNA of XIAP. miRNAs are known to suppress the expression of mRNA targets [43]. Indeed, we found that miR-122 overexpression led to reduced expression of XIAP in HAECs, and conversely, miR-122 knockdown caused an increased expression of XIAP, at both mRNA (Fig. 4D) and protein levels (Fig. 4E). Furthermore, in vivo, contrary to the elevated expression of miR-122, XIAP expression was significantly decreased in aortic ECs from ApoE$^{-/-}$ mice fed HFD (Fig. 4F). Taken together, these lines of evidence illustrate that miR-122 directly targets and suppresses XIAP expression in ECs, which may be associated with induced EC apoptosis in atherosclerosis.

3.5. XIAP suppression mediates the pro-apoptotic role of miR-122 in ox-LDL-treated HAECs

At last, to clarify whether the regulation of XIAP contributes to miR-122 knockdown-attenuated apoptosis in HAECs under ox-LDL treatment, we depleted XIAP expression through transfecting specific small interfering RNA (siRNA). Consistently, as a target of miR-122, XIAP expression was increased in ox-LDL-treated HAECs by miR-122 inhibition (Fig. 5A, lane 1 vs. lane 2). Further, compared with scrambled control siRNA (siCtrl), the transfection of siRNA targeting XIAP (siXIAP) resulted in efficient depletion of XIAP (Fig. 5A, lane 3 vs. lane 4). Strikingly, TUNEL assay showed that miR-122 knockdown-attenuated apoptosis in HAECs was completely recovered along with XIAP depletion (Fig. 5B), indicating that this anti-apoptotic role is dependent on XIAP upregulation. Moreover, this concept was further supported by the recovered expression of cleaved caspase-3 when XIAP was depleted, as analyzed by Western blotting assay (Fig. 5C). Thus, these mechanistic studies show that the functional role of miR-122 in ox-LDL-induced apoptosis in HAECs is dependent on its suppressive regulation of XIAP.

4. Discussion

It has long been recognized that EC apoptosis plays several detrimental roles in the pathogenesis of atherosclerosis [44,45]. Therefore, the development of strategies for preventing or reducing EC apoptosis would provide clinical benefit in modifying the progression of

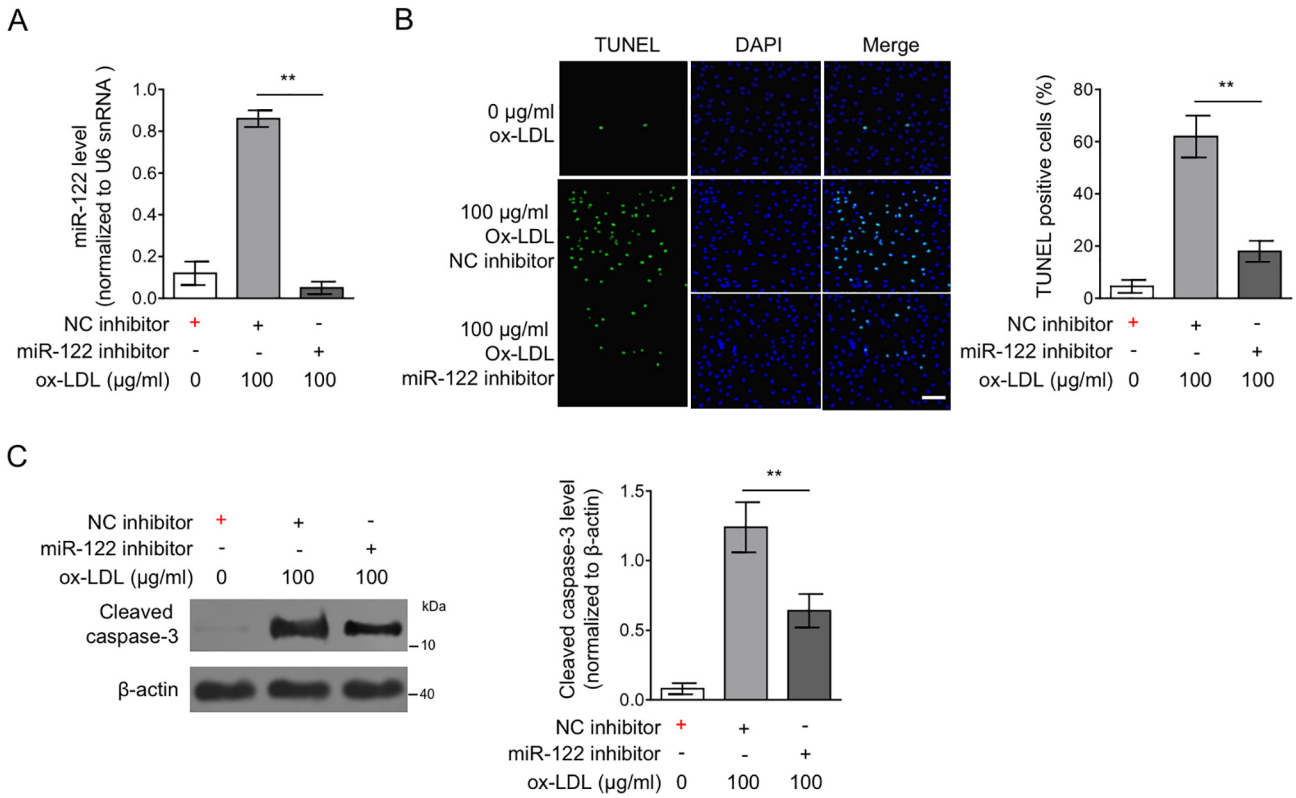

Fig. 3. miR-122 knockdown suppresses ox-LDL-induced apoptosis of HAECs.
(**A–C**) HAECs were transfected with negative control (NC) inhibitor or miR-122 inhibitor. One day after transfection, HAECs were further treated with or without 100 μg/ml ox-LDL for 2 days as indicated. (**A**) miR-122 expression was determined by qRT-PCR analysis. U6 snRNA was used as a reference control. Data are expressed as mean ± SD (n = 3). (**B**) The apoptosis of HAECs was measured by TUNEL staining. The representative images (left) and quantification analysis (right) of the percentage of TUNEL positive cells are shown. Nuclei were stained blue with DAPI. Data are expressed as mean ± SD ($n = 15$). Scale bar, 100 μM. (**C**) The protein expression of cleaved caspase-3 was determined by Western blotting analysis. β-actin was used as a loading control. The level of cleaved caspase-3 expression was quantified. Data are expressed as mean ± SD (n = 3). Student's *t*-test. $^{**}P < 0.01$ vs. NC. (For interpretation of the references to colour in this figure legend, the reader is referred to the web version of this article.)

atherosclerosis. Whereas, the molecular mechanisms leading to EC apoptosis are not well understood, which impedes the development of targeted therapies. In recent years, miRNAs are emerging as important regulators of atherosclerosis-associated EC apoptosis [46–49]. But, to date, our understanding of the regulation of EC apoptosis by miRNAs is still limited. In the current study, we uncover a novel role of miR-122 in promoting ox-LDL-induced EC apoptosis by directly targeting XIAP, which may offer a therapeutic implication for intervening atherosclerosis or other associated vascular diseases through reducing EC apoptosis.

The biological function of miR-122 is often referred to the regulation of hepatic physiology and pathology, including lipid metabolism, hepatocellular carcinoma (HCC) and hepatitis C infection [50,51]. The downregulation of miR-122 is frequently present in human HCC, and the restored expression of miR-122 suppresses the growth, induces cell cycle arrest and promotes apoptosis of HCC cells [20,52,53]. Although miR-122 is considered to be a liver-specific miRNA, its role has recently been extended to other circumstances, such as activating p53 translation in primary fibroblasts [54], ameliorating intestinal epithelial cell injury in Crohn's disease [55], suppressing aggressive phenotypes in breast cancer [56], glioma [57] and non-small-cell lung cancer cells [58], and impeding angiogenic properties of endothelial cells [59]. These findings indicate that miR-122 participates in a broad range of activities which are beyond previously thought. Due to the positive regulation of miR-122 in ox-LDL-induced apoptosis revealed in our study, it is very likely that the upregulated miR-122 would aggravate ox-LDL-induced apoptosis, which could create a positive feed-back loop between miR-122 upregulation and EC apoptosis. As far as we know, this is the first time that miR-122 is positively connected to EC apoptosis in the context of atherosclerosis, therefore extending its functional role to atherosclerosis pathology. Yet how exactly the expression of miR-122 is controlled remains largely unclear. Three major mechanisms performing at different levels including transcription, processing and post-synthesis 3′-uridylation modification are supposed to regulate miR-122 [60]. Further studies would be required to address the regulatory mechanisms of miR-122 expression in ECs in response to atherogenic stimuli.

As known, young ApoE$^{-/-}$ mice develop spontaneous atherosclerotic lesions even on a ND in a time-dependent manner [25,61], which means that compared with wild-type mice, the baseline levels of atherosclerotic severity and apoptosis in aortic ECs would be higher in ApoE$^{-/-}$ mice fed a ND. Notably, ApoE$^{-/-}$ mice fed a ND displayed a certain degree of apoptotic cells and expression of cleaved caspase-3, although largely lower than those fed a HFD (Fig. 1), presumably suggesting that in these mice, early signs of spontaneous atherosclerosis have already appeared. However, it should be noted that in animal experiments, we did not synchronously analyze wild-type mice because of intended experimental purposes, which undoubtedly limits our understanding of the baseline expression and functional results of miR-122 in mice. Relevant animal studies are required to fully address this issue in the future.

The physiologic concentration of ox-LDL is around 5 μg/ml [62]. It's known that Ox-LDL induces apoptosis in a concentration dependent manner in the cells [63]. Previous studies have shown that low physiologic concentrations of ox-LDL (< 5 μg protein/ml) not only do not cause apoptosis, but are associated with endothelial cell proliferation

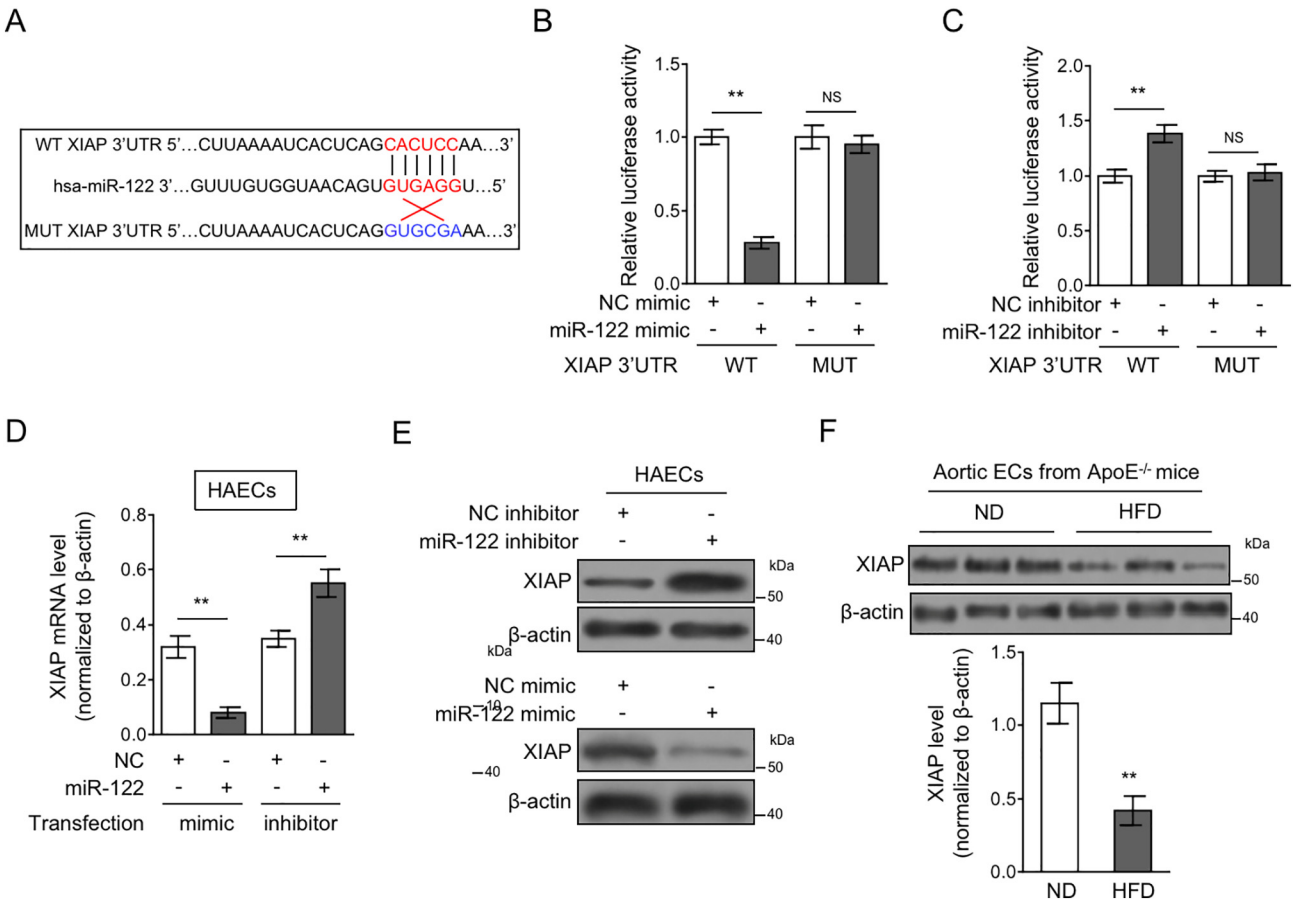

Fig. 4. miR-122 directly targets XIAP in HAECs.
(**A**) Sequence alignment of miR-122 and 3′UTR of XIAP, which shows the complementarity (matched bases marked in red letters). The mutant sites are also shown. (**B**) Luciferase activity of wild-type (WT) or mutant (MUT) 3′UTR of XIAP in HEK293 cells transfected with negative control (NC) mimic or miR-122 mimic for 2 days. (**C**) Luciferase activity of WT or MUT 3′UTR of XIAP in HEK293 cells transfected with NC inhibitor or miR-122 inhibitor for 2 days. (**D–E**) HAECs were transfected with NC mimic, miR-122 mimic, NC inhibitor, or miR-122 inhibitor for 2 days. (**D**) XIAP mRNA expression was determined by qRT-PCR analysis. β-actin was used as a reference control. (**E**) XIAP protein expression was determined by Western blotting analysis. β-actin was used as a loading control. Representative images from 3 independent assays are depicted. (**F**) HAECs isolated from the aortic intima of ApoE$^{-/-}$ mice fed a HFD or normal diet for 16 weeks were analyzed by Western blotting to determine XIAP protein expression. β-actin was used as a loading control. Blot images were representative of 3 mice in each group. The quantification analysis of XIAP expression is shown below. Data are expressed as mean ± SD (n = 3). Student's *t*-test. $^{**}P < 0.01$; NS, not significant. (For interpretation of the references to colour in this figure legend, the reader is referred to the web version of this article.)

[64,65]. But, on the other hand, higher concentrations (30–50 μg/ml) have been shown to reduce the viability of vascular cells and induce cell apoptosis [66,67]. In the current study, we established an in vitro apoptosis model of HAECs by treating them with 25, 50, and 100 μg/ml ox-LDL, which exceed the physiologic range. These concentrations of ox-LDL were also used in many other studies reported by other groups [18,68–71]. Although our cell culture studies may indeed bear only partial relevance to pathophysiological mechanisms present in vivo, they possess important implications for understanding the relation between ox-LDL-induced HAECs apoptosis and miR-122.

XIAP belongs to IAP proteins and is the exclusive endogenous mammalian inhibitor of caspases that inhibits the execution of apoptosis through binding active caspases 3 and 7 with its BIR2 domain and the linker region domain, and binding the processed caspase-9 with its BIR3 domain [72]. Consistently, the transgenic overexpression of XIAP protects against caspase activation and tissue death following neonatal hypoxia-ischemia [73], and reversely, the loss of XIAP or deletion of RING domain causes excessive cell death [74]. We noticed decreased expression of XIAP in aortic ECs from ApoE$^{-/-}$ mice fed HFD, implying that the XIAP-conferred anti-apoptotic machinery may be impaired in aortic ECs in the development of atherosclerosis, whereby promoting the apoptosis of aortic ECs. In agreement with XIAP negative regulation of EC apoptosis, we demonstrate that as a direct target of miR-122, the relieved suppressive regulation of XIAP expression upon miR-122 knockdown accounts for the attenuated ox-LDL-induced apoptosis in HAECs, which underscores a critical role of miR-122/XIAP axis in the regulation of EC apoptosis. Coincidently, miR-122 was also reported to target XIAP in colorectal cancer cells [75]. Mechanistically, we found that the expression of cleaved caspase-3 was increased when XIAP was silenced by siRNA, therefore, at least suggesting that the inhibition of caspases 3 cleavage is one of the major mechanisms that could explain its anti-apoptotic role in ECs. It's noteworthy that in addition to XIAP, other downstream targets of miR-122 have been reported to mediate its regulatory role in apoptosis, albeit under different circumstances, such as DJ-1 [76], RUNX2 [77], Bcl-w [78] and GATA-4 [41]. It is interesting to examine whether these targets contribute to miR-122 regulation of EC apoptosis. Addressing this issue could provide useful hint to advance our understanding of miR-122 function involved in the pathogenesis of atherosclerosis.

Funding

This study was supported by Project of Tianjin Chest Hospital (2018XKZ15).

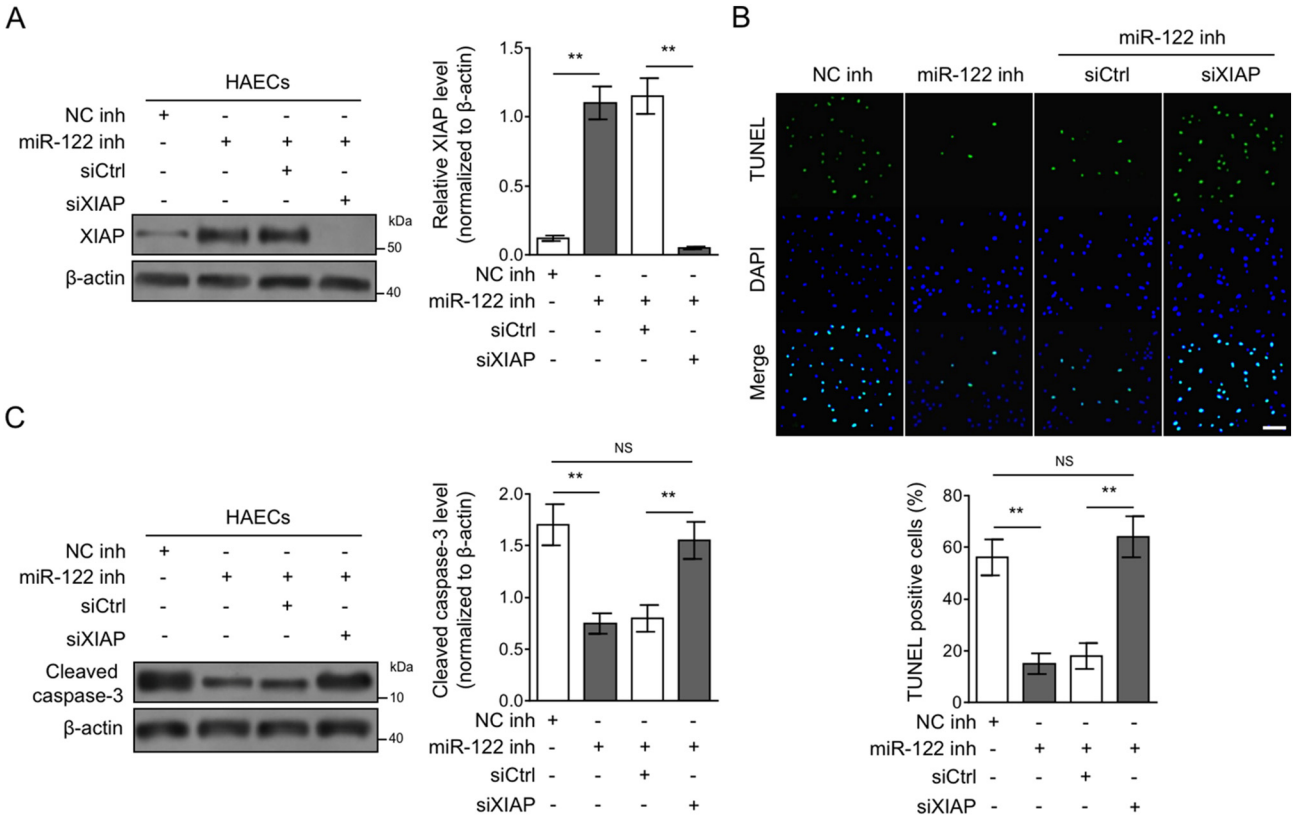

Fig. 5. miR-122 knockdown-suppressed ox-LDL-induced apoptosis of HAECs relies on upregulating XIAP.
(**A–C**) HAECs were cotransfected siRNA control (siCtrl) or siRNA XIAP (siXIAP) with NC inhibitor (inh) or miR-122 inh. One day after transfection, HAECs were further treated with 100 μg/ml ox-LDL for 2 days. (**A**) The protein expression of XIAP was determined by Western blotting analysis. β-Actin was used as a loading control. Representative images from 3 independent assays are depicted. The quantification analysis of XIAP expression is shown right. Data are expressed as mean ± SD (n = 3). (**B**) The apoptosis of HAECs was measured by TUNEL staining. The representative images (left) and quantification analysis (right) of the percentage of TUNEL positive cells are shown. Nuclei were stained blue with DAPI. Data are expressed as mean ± SD (n = 15). Scale bar, 100 μM. (**C**) The protein expression of cleaved caspase-3 was determined by Western blotting analysis. β-Actin was used as a loading control. Representative images from 3 independent assays are depicted. The quantification analysis of cleaved caspase-3 expression is shown right. Data are expressed as mean ± SD (n = 3). One-way ANOVA followed by post-hoc Turkey's test. $^{**}P < 0.01$; NS, not significant. (For interpretation of the references to colour in this figure legend, the reader is referred to the web version of this article.)

Declaration of Competing Interest

None.

References

[1] I. Tabas, G. Garcia-Cardena, G.K. Owens, Recent insights into the cellular biology of atherosclerosis, J. Cell Biol. 209 (2015) 13–22.
[2] J. Viola, O. Soehnlein, Atherosclerosis - a matter of unresolved inflammation, Semin. Immunol. 27 (2015) 184–193.
[3] M.A. Gimbrone Jr., G. Garcia-Cardena, Endothelial cell dysfunction and the pathobiology of atherosclerosis, Circ. Res. 118 (2016) 620–636.
[4] G. Chinetti-Gbaguidi, S. Colin, B. Staels, Macrophage subsets in atherosclerosis, Nat. Rev. Cardiol. 12 (2015) 10–17.
[5] D.A. Chistiakov, A.N. Orekhov, Y.V. Bobryshev, Vascular smooth muscle cell in atherosclerosis, Acta Physiol. 214 (2015) 33–50.
[6] D. Tousoulis, E. Oikonomou, E.K. Economou, F. Crea, J.C. Kaski, Inflammatory cytokines in atherosclerosis: current therapeutic approaches, Eur. Heart J. 37 (2016) 1723–1732.
[7] G. Foteinos, A.R. Afzal, K. Mandal, M. Jahangiri, Q. Xu, Anti-heat shock protein 60 autoantibodies induce atherosclerosis in apolipoprotein E-deficient mice via endothelial damage, Circulation 112 (2005) 1206–1213.
[8] N. Peng, N. Meng, S. Wang, F. Zhao, J. Zhao, L. Su, et al., An activator of mTOR inhibits oxLDL-induced autophagy and apoptosis in vascular endothelial cells and restricts atherosclerosis in apolipoprotein E(−)/(−) mice, Sci. Rep. 4 (2014) 5519.
[9] C. Sun, M.H. Wu, S.Y. Yuan, Nonmuscle myosin light-chain kinase deficiency attenuates atherosclerosis in apolipoprotein E-deficient mice via reduced endothelial barrier dysfunction and monocyte migration, Circulation 124 (2011) 48–57.
[10] A.V. Sima, C.S. Stancu, M. Simionescu, Vascular endothelium in atherosclerosis, Cell Tissue Res. 335 (2009) 191–203.
[11] Z. Mallat, A. Tedgui, Apoptosis in the vasculature: mechanisms and functional importance, Br. J. Pharmacol. 130 (2000) 947–962.
[12] S. Paone, A.A. Baxter, M.D. Hulett, I.K.H. Poon, Endothelial cell apoptosis and the role of endothelial cell-derived extracellular vesicles in the progression of atherosclerosis, Cell. Mol. Life Sci. 76 (6) (2018) 1093–1106.
[13] N. Bushati, S.M. Cohen, microRNA functions, Annu. Rev. Cell Dev. Biol. 23 (2007) 175–205.
[14] J. Madrigal-Matute, N. Rotllan, J.F. Aranda, C. Fernandez-Hernando, MicroRNAs and atherosclerosis, Curr. Atheroscler. Rep. 15 (2013) 322.
[15] A. Schober, C. Weber, Mechanisms of MicroRNAs in atherosclerosis, Annu. Rev. Pathol. 11 (2016) 583–616.
[16] B. Qin, B. Xiao, D. Liang, J. Xia, Y. Li, H. Yang, MicroRNAs expression in ox-LDL treated HUVECs: MiR-365 modulates apoptosis and Bcl-2 expression, Biochem. Biophys. Res. Commun. 410 (2011) 127–133.
[17] T. Zhang, F. Tian, J. Wang, J. Jing, S.S. Zhou, Y.D. Chen, Atherosclerosis-associated endothelial cell apoptosis by MiR-429-mediated down regulation of Bcl-2, Cell. Physiol. Biochem. 37 (2015) 1421–1430.
[18] Y. Zhang, W. Qin, L. Zhang, X. Wu, N. Du, Y. Hu, et al., MicroRNA-26a prevents endothelial cell apoptosis by directly targeting TRPC6 in the setting of atherosclerosis, Sci. Rep. 5 (2015) 9401.
[19] B. Qin, B. Xiao, D. Liang, Y. Li, T. Jiang, H. Yang, MicroRNA let-7c inhibits Bcl-xl expression and regulates ox-LDL-induced endothelial apoptosis, BMB Rep. 45 (2012) 464–469.
[20] L. Ma, J. Liu, J. Shen, L. Liu, J. Wu, W. Li, et al., Expression of miR-122 mediated by adenoviral vector induces apoptosis and cell cycle arrest of cancer cells, Cancer Biol. Ther. 9 (2010) 554–561.
[21] V. Manfe, E. Biskup, A. Rosbjerg, M. Kamstrup, A.G. Skov, C.M. Lerche, et al., miR-122 regulates p53/Akt signalling and the chemotherapy-induced apoptosis in cutaneous T-cell lymphoma, PLoS One 7 (2012) e29541.
[22] Z.J. Pei, Z.G. Zhang, A.X. Hu, F. Yang, Y. Gai, miR-122-5p inhibits tumor cell proliferation and induces apoptosis by targeting MYC in gastric cancer cells, Pharmazie 72 (2017) 344–347.
[23] Z.W. Zhang, H. Li, S.S. Chen, Y. Li, Z.Y. Cui, J. Ma, MicroRNA-122 regulates caspase-8 and promotes the apoptosis of mouse cardiomyocytes, Braz. J. Med. Biol.

Res. 50 (2017) (e 5760.
[24] J. Poirier, J. Davignon, D. Bouthillier, S. Kogan, P. Bertrand, S. Gauthier, Apolipoprotein E polymorphism and Alzheimer's disease, Lancet 342 (1993) 697–699.
[25] Y. Nakashima, A.S. Plump, E.W. Raines, J.L. Breslow, R. Ross, ApoE-deficient mice develop lesions of all phases of atherosclerosis throughout the arterial tree, Arterioscler. Thromb. 14 (1994) 133–140.
[26] N. Komura, N. Maeda, T. Mori, S. Kihara, H. Nakatsuji, A. Hirata, et al., Adiponectin protein exists in aortic endothelial cells, PLoS One 8 (2013) e71271.
[27] A. Li, W. Song, J. Qian, Y. Li, J. He, Q. Zhang, et al., MiR-122 modulates type I interferon expression through blocking suppressor of cytokine signaling 1, Int. J. Biochem. Cell Biol. 45 (2013) 858–865.
[28] K.J. Livak, T.D. Schmittgen, Analysis of relative gene expression data using real-time quantitative PCR and the 2(-Delta Delta C(T)) Method, Methods. 25 (2001) 402–408.
[29] J. Qian, A. Zhai, W. Kao, Y. Li, W. Song, Y. Fu, et al., Modulation of miR-122 on persistently Borna disease virus infected human oligodendroglial cells, Antivir. Res. 87 (2010) 249–256.
[30] Y. Yang, L. Yang, X. Liang, G. Zhu, MicroRNA-155 promotes atherosclerosis inflammation via targeting SOCS1, Cell. Physiol. Biochem. 36 (2015) 1371–1381.
[31] C.A. Schneider, W.S. Rasband, K.W. Eliceiri, NIH image to ImageJ: 25 years of image analysis, Nat. Methods 9 (2012) 671–675.
[32] K. Kyrylkova, S. Kyryachenko, M. Leid, C. Kioussi, Detection of apoptosis by TUNEL assay, Methods Mol. Biol. 887 (2012) 41–47.
[33] G.B. Sun, M. Qin, J.X. Ye, R.L. Pan, X.B. Meng, M. Wang, et al., Inhibitory effects of myricitrin on oxidative stress-induced endothelial damage and early atherosclerosis in ApoE−/− mice, Toxicol. Appl. Pharmacol. 271 (2013) 114–126.
[34] L. Zhang, H. Cheng, Y. Yue, S. Li, D. Zhang, R.T.U.G. He, 1 knockdown ameliorates atherosclerosis via up-regulating the expression of miR-133a target gene FGF1, Cardiovasc. Pathol. 33 (2018) 6–15.
[35] T.L. Huber, V. Kouskoff, H.J. Fehling, J. Palis, G. Keller, Haemangioblast commitment is initiated in the primitive streak of the mouse embryo, Nature 432 (2004) 625–630.
[36] C. Napoli, I. Martin-Padura, F. de Nigris, M. Giorgio, G. Mansueto, P. Somma, et al., Deletion of the p66Shc longevity gene reduces systemic and tissue oxidative stress, vascular cell apoptosis, and early atherogenesis in mice fed a high-fat diet, Proc. Natl. Acad. Sci. U. S. A. 100 (2003) 2112–2116.
[37] H.Q. Zhu, Q. li, L.Y. Dong, Q. Zhou, H. Wang, Y. Wang, MicroRNA-29b promotes high-fat diet-stimulated endothelial permeability and apoptosis in apoE knock-out mice by down-regulating MT1 expression, Int. J. Cardiol. 176 (2014) 764–770.
[38] A.G. Porter, R.U. Janicke, Emerging roles of caspase-3 in apoptosis, Cell Death Differ. 6 (1999) 99–104.
[39] M. Harada-Shiba, M. Kinoshita, H. Kamido, K. Shimokado, Oxidized low density lipoprotein induces apoptosis in cultured human umbilical vein endothelial cells by common and unique mechanisms, J. Biol. Chem. 273 (1998) 9681–9687.
[40] Y.S. Hsieh, W.H. Kuo, T.W. Lin, H.R. Chang, T.H. Lin, P.N. Chen, et al., Protective effects of berberine against low-density lipoprotein (LDL) oxidation and oxidized LDL-induced cytotoxicity on endothelial cells, J. Agric. Food Chem. 55 (2007) 10437–10445.
[41] W. Liang, J. Guo, J. Li, C. Bai, Y. Dong, Downregulation of miR-122 attenuates hypoxia/reoxygenation (H/R)-induced myocardial cell apoptosis by upregulating GATA-4, Biochem. Biophys. Res. Commun. 478 (2016) 1416–1422.
[42] L.M. Martins, I. Iaccarino, T. Tenev, S. Gschmeissner, N.F. Totty, N.R. Lemoine, et al., The serine protease Omi/HtrA2 regulates apoptosis by binding XIAP through a reaper-like motif, J. Biol. Chem. 277 (2002) 439–444.
[43] V. Ambros, The functions of animal microRNAs, Nature 431 (2004) 350–355.
[44] J.C. Choy, D.J. Granville, D.W. Hunt, B.M. McManus, Endothelial cell apoptosis: biochemical characteristics and potential implications for atherosclerosis, J. Mol. Cell. Cardiol. 33 (2001) 1673–1690.
[45] M. Mudau, A. Genis, A. Lochner, H. Strijdom, Endothelial dysfunction: the early predictor of atherosclerosis, Cardiovasc. J. Afr. 23 (2012) 222–231.
[46] Y. Li, C. Yang, L. Zhang, P. Yang, MicroRNA-210 induces endothelial cell apoptosis by directly targeting PDK1 in the setting of atherosclerosis, Cell. Mol. Biol. Lett. 22 (2017) 3.
[47] B. Qin, Y. Shu, L. Long, H. Li, X. Men, L. Feng, et al., MicroRNA-142-3p induces atherosclerosis-associated endothelial cell apoptosis by directly targeting rictor, Cell. Physiol. Biochem. 47 (2018) 1589–1603.
[48] K. Xu, P. Liu, Y. Zhao, Upregulation of microRNA-876 induces endothelial cell apoptosis by suppressing Bcl-xl in development of atherosclerosis, Cell. Physiol. Biochem. 42 (2017) 1540–1549.
[49] J. Zhao, S.L. Ou, W.Y. Wang, C. Yan, L.X. Chi, MicroRNA-1907 enhances atherosclerosis-associated endothelial cell apoptosis by suppressing Bcl-2, Am. J. Transl. Res. 9 (2017) 3433–3442.
[50] C. Esau, S. Davis, S.F. Murray, X.X. Yu, S.K. Pandey, M. Pear, et al., miR-122 regulation of lipid metabolism revealed by in vivo antisense targeting, Cell Metab. 3 (2006) 87–98.
[51] W. Filipowicz, H. Grosshans, The liver-specific microRNA miR-122: biology and therapeutic potential, Prog. Drug Res. 67 (2011) 221–238.
[52] H. Kutay, S. Bai, J. Datta, T. Motiwala, I. Pogribny, W. Frankel, et al., Downregulation of miR-122 in the rodent and human hepatocellular carcinomas, J. Cell. Biochem. 99 (2006) 671–678.
[53] C.J. Lin, H.Y. Gong, H.C. Tseng, W.L. Wang, J.L. Wu, miR-122 targets an anti-apoptotic gene, Bcl-w, in human hepatocellular carcinoma cell lines, Biochem. Biophys. Res. Commun. 375 (2008) 315–320.
[54] D.M. Burns, A. D'Ambrogio, S. Nottrott, J.D. Richter, CPEB and two poly(A) polymerases control miR-122 stability and p53 mRNA translation, Nature 473 (2011) 105–108.
[55] Y. Chen, C. Wang, Y. Liu, L. Tang, M. Zheng, C. Xu, et al., miR-122 targets NOD2 to decrease intestinal epithelial cell injury in Crohn's disease, Biochem. Biophys. Res. Commun. 438 (2013) 133–139.
[56] B. Wang, H. Wang, Z. Yang, MiR-122 inhibits cell proliferation and tumorigenesis of breast cancer by targeting IGF1R, PLoS One 7 (2012) e47053.
[57] G. Wang, Y. Zhao, Y. Zheng, MiR-122/Wnt/beta-catenin regulatory circuitry sustains glioma progression, Tumour Biol. 35 (2014) 8565–8572.
[58] H. Qin, J. Sha, C. Jiang, X. Gao, L. Qu, H. Yan, et al., miR-122 inhibits metastasis and epithelial-mesenchymal transition of non-small-cell lung cancer cells, Onco Targets Ther. 8 (2015) 3175–3184.
[59] S. Bai, M.W. Nasser, B. Wang, S.H. Hsu, J. Datta, H. Kutay, et al., MicroRNA-122 inhibits tumorigenic properties of hepatocellular carcinoma cells and sensitizes these cells to sorafenib, J. Biol. Chem. 284 (2009) 32015–32027.
[60] A.P. Lewis, C.L. Jopling, Regulation and biological function of the liver-specific miR-122, Biochem. Soc. Trans. 38 (2010) 1553–1557.
[61] R.L. Reddick, S.H. Zhang, N. Maeda, Atherosclerosis in mice lacking apo E. Evaluation of lesional development and progression, Arterioscler. Thromb. 14 (1994) 141–147.
[62] M. Khaidakov, S. Mitra, X. Wang, Z. Ding, N. Bora, V. Lyzogubov, et al., Large impact of low concentration oxidized LDL on angiogenic potential of human endothelial cells: a microarray study, PLoS One 7 (2012) e47421.
[63] E. Nishio, S. Arimura, Y. Watanabe, Oxidized LDL induces apoptosis in cultured smooth muscle cells: a possible role for 7-ketocholesterol, Biochem. Biophys. Res. Commun. 223 (1996) 413–418.
[64] S. Chatterjee, Role of oxidized human plasma low density lipoproteins in atherosclerosis: effects on smooth muscle cell proliferation, Mol. Cell. Biochem. 111 (1992) 143–147.
[65] S. Seibold, D. Schurle, A. Heinloth, G. Wolf, M. Wagner, J. Galle, Oxidized LDL induces proliferation and hypertrophy in human umbilical vein endothelial cells via regulation of p27Kip1 expression: role of RhoA, J. Am. Soc. Nephrol. 15 (2004) 3026–3034.
[66] R. Li, D. Mittelstein, K. Fang, T. Beebe, K. Quigley, J. Berliner, et al., Angiopoeitin-2 modulates Survivin expression in OxLDL-induced endothelial cell apoptosis, Biochem. Biophys. Res. Commun. 417 (2012) 619–622.
[67] M.D. Mattaliano, C. Huard, W. Cao, A.A. Hill, W. Zhong, R.V. Martinez, et al., LOX-1-dependent transcriptional regulation in response to oxidized LDL treatment of human aortic endothelial cells, Am. J. Physiol. Cell Physiol. 296 (2009) C1329–C1337.
[68] C. Claise, M. Edeas, N. Chaouchi, J. Chalas, L. Capel, S. Kalimouttou, et al., Oxidized-LDL induce apoptosis in HUVEC but not in the endothelial cell line EA.hy 926, Atherosclerosis 147 (1999) 95–104.
[69] D. Namgaladze, A. Kollas, B. Brune, Oxidized LDL attenuates apoptosis in monocytic cells by activating ERK signaling, J. Lipid Res. 49 (2008) 58–65.
[70] X. Wang, J. Chen, Q. Tao, J. Zhu, Y. Shang, Effects of ox-LDL on number and activity of circulating endothelial progenitor cells, Drug Chem. Toxicol. 27 (2004) 243–255.
[71] B.C. Zhang, C.W. Zhang, C. Wang, D.F. Pan, T.D. Xu, D.Y. Li, Luteolin attenuates foam cell formation and apoptosis in Ox-LDL-stimulated macrophages by enhancing autophagy, Cell. Physiol. Biochem. 39 (2016) 2065–2076.
[72] D. Vucic, XIAP at the crossroads of cell death and inflammation, Oncotarget 9 (2018) 27319–27320.
[73] X. Wang, C. Zhu, X. Wang, H. Hagberg, L. Korhonen, M. Sandberg, et al., X-linked inhibitor of apoptosis (XIAP) protein protects against caspase activation and tissue loss after neonatal hypoxia-ischemia, Neurobiol. Dis. 16 (2004) 179–189.
[74] M. Yabal, N. Muller, H. Adler, N. Knies, C.J. Gross, R.B. Damgaard, et al., XIAP restricts TNF- and RIP3-dependent cell death and inflammasome activation, Cell Rep. 7 (2014) 1796–1808.
[75] Y. Hua, Y. Zhu, J. Zhang, Z. Zhu, Z. Ning, H. Chen, et al., miR-122 targets X-linked inhibitor of apoptosis protein to sensitize oxaliplatin-resistant colorectal cancer cells to oxaliplatin-mediated cytotoxicity, Cell. Physiol. Biochem. 51 (2018) 2148–2159.
[76] X.H. Qu, K. Zhang, MiR-122 regulates cell apoptosis and ROS by targeting DJ-1 in renal ischemic reperfusion injury rat models, Eur. Rev. Med. Pharmacol. Sci. 22 (2018) 8830–8838.
[77] C.Q. Ding, W.S. Deng, X.F. Yin, X.D. Ding, MiR-122 inhibits cell proliferation and induces apoptosis by targeting runt-related transcription factors 2 in human glioma, Eur. Rev. Med. Pharmacol. Sci. 22 (2018) 4925–4933.
[78] Y.H. Cui, H.Y. Li, Z.X. Gao, N. Liang, S.S. Ma, F.J. Meng, et al., Regulation of apoptosis by miR-122 in pterygium via targeting Bcl-w, Invest. Ophthalmol. Vis. Sci. 57 (2016) 3723–3730.